Journal of
Synchrotron Radiation

ISSN 0909-0495

Received 16 March 2007
Accepted 8 August 2007

A multi-sample automatic system for *in situ* electrochemical X-ray diffraction synchrotron measurements

Fabio Rosciano,* Michael Holzapfel,‡ Hermann Kaiser, Werner Scheifele, Patrick Ruch, Matthias Hahn, Rüdiger Kötz and Petr Novák

Paul Scherrer Institut, Electrochemistry Laboratory, CH-5232 Villigen PSI, Switzerland.
E-mail: fabio.rosciano@psi.ch

An automatic system that allows continuous *in situ* electrochemical X-ray diffraction measurements has been developed and implemented at the MS-X04SA beamline at the Swiss Light Source. The system consists of an automatic sample changer, improved 'coffee bag' electrochemical cells, and simple control software. The sample changer can sequentially move up to 32 electrochemical cells into the beam. For each cell an independent electrochemical program is possible. The MYTHEN microstrip detector at the beamline enables parallel detection of diffracted X-ray beams and, thus, fast data acquisition, along with a high 2θ resolution. In this communication the set-up is presented on two typical examples from the field of lithium-ion batteries, (i) structural changes in a layered $LiCoO_2$ positive electrode upon battery charging and (ii) the effect of co-intercalation of ionic liquids into the graphite negative electrode.

© 2007 International Union of Crystallography
Printed in Singapore – all rights reserved

Keywords: *in situ* X-ray diffraction; lithium-ion batteries; ionic liquids; electrochemistry.

1. Introduction

Portable power sources have undergone a quick evolution in the last decade, leading to smaller and more efficient devices for various applications ranging from personal electronic gadgets to hybrid vehicles. Among these, lithium-ion batteries are prominent for their ability to deliver both high power and high energy density (Tarascon & Armand, 2001). Lithium-ion batteries work on the following principle: both the anode and the cathode are based on host materials (often layered oxide structures) allowing reversible intercalation and deintercalation of lithium ions (Nishi, 2001). The understanding of structural changes in these intercalation materials is an important prerequisite for the further improvement of the battery electrodes. An excellent method for studying the materials' structural changes during electrochemical cycling is X-ray diffraction (XRD). Most of the relevant materials are sensitive to humidity and/or air when partly charged (Winter *et al.*, 1998). Thus, *in situ* experiments in hermetically sealed electrochemical cells are advantageous and usually necessary. Implementing the *in situ* cells at a synchrotron will allow for the required fast measurements with high resolution, qualities that cannot be achieved on conventional X-ray diffractometers.

Only few *in situ* electrochemical cells for XRD measurements have been described over the years. Our particular implementation is derived from the set-up known as 'coffee bag' cells (Gustafson *et al.*, 1992) which has important advantages over other approaches, namely the use of cheap single-use components, easy fabrication of the cells, and good reproducibility of the electrochemical measurements. The main innovation in our new system presented here is the automatic sample changer: the collection of diffraction patterns at the Material Science (MS) beamline at the Swiss Light Source (SLS) is very fast ($\sim$10 s), thus, for an efficient use of the costly beam time, many samples are automatically measured quasi in parallel. The time-consuming manual manipulations in the hatch are no longer necessary. (Note that electrochemical experiments are carried out on a time scale of hours.) The electrochemical cells are sequentially and repeatedly moved into the X-ray beam in a very precise and reproducible manner and the X-ray patterns are recorded as a function of either time or any other electrochemical parameter like cell voltage or the amount of charge given to the battery.

2. Experimental set-up

The strength of the system is the tight integration of every component in the final design. The electrochemical cells have been engineered to provide stable electrochemical performance while minimizing unwanted effects on XRD measurements, especially strong X-ray absorption. The sample changer has been designed to fit in the beamline experimental hutch

‡ Present address: Süd-Chemie AG, Ostenrieder Strasse 15, D-85368 Moosburg, Germany.

and has been kept as simple as possible to reduce the risk for maintenance. The electrochemical measurements are automatically controlled by the battery cycling system from Astrol Electronic AG (Oberrohrdorf, Switzerland; http://www.astrol.ch/) which features easy programming and flexibility while running.

2.1. Electrochemical cells

The 'coffee bag' electrochemical cells (Gustafson *et al.*, 1992; Tarascon *et al.*, 1996) consist of several flat parts designed to keep the thickness of the assembled cell in the order of 500 µm while minimizing the presence of materials, other than the active material, giving rise to X-ray reflexes. In Fig. 1 a schematic drawing of the cell is shown.

Most components of a lithium-ion battery are very sensitive to oxygen and moisture, thus the strictest requirement on the *in situ* cell is the need for air and moisture tightness. For this reason the cells are sealed with a 167 µm-thick composite foil constituted by four layers: from the inside to the outside (i) polyethylene (PE), (ii) aluminium, (iii) PE and (iv) oriented polyamide (OPA). The PE layer is thermosealable while the OPA layer is not, thus being on the outside of every cell. The 12 µm-thick aluminium inner layer is a good (and necessary) barrier to O_2 and H_2O. Of course, the use of such a composite foil introduces additional features in the XRD patterns but it is our preferred solution compared with standard *in situ* XRD cells using beryllium windows practically transparent to X-rays; apart from the health hazard of beryllium, corrosion of beryllium occurs at potentials positive to 4 V *versus* Li/Li^+.

The electroactive mass is supported by a current collector made from expanded metal (Al or Cu, depending on the working potential window of the particular material). The electrodes are prepared by the common 'doctor blade' technique which consists of spreading a slurry in (an) organic solvent(s) of the electroactive material, a conductivity enhancer (graphite and/or carbon black) and a binder (*e.g.* PVdF). The slurry is first spread onto a non-adhesive sheet from which it is easily removed once dried. The free-standing electrodes (2 cm × 2 cm) are cut with a scalpel and then pressed on the respective current collectors. All cell components are then dried in vacuum at 393 K overnight to remove all traces of solvents and humidity and subsequently transferred into an Ar-filled glove box. In the glove box the cells are assembled, filled with the electrolyte, and then sealed using a home-made machine that evacuates the cell and thermally seals the foil. For experiments where the electrolyte amount is an important variable and/or when the electrolyte is too volatile, the alternative is to seal dry cells with a straw which is later used to fill-in the electrolyte and then sealed manually. In Fig. 2 the two cell types (with and without a straw) are shown.

A commercial polymeric separator (Celgard) was normally used because of its low thickness and good electrochemical performance. A drawback of this material is the low amount of electrolyte that it can absorb; if more electrolyte is needed, a glass fiber separator can be used. Of course, the separator may contribute to the XRD patterns; however, this has not been a problem within the measurements described below.

Prior to being introduced into the sample changer, each cell is enclosed in a special holder that keeps it in the correct position (*i.e.* the active material is aligned with the beam). The holder is shown in Fig. 3. The casing is closed with screws; this

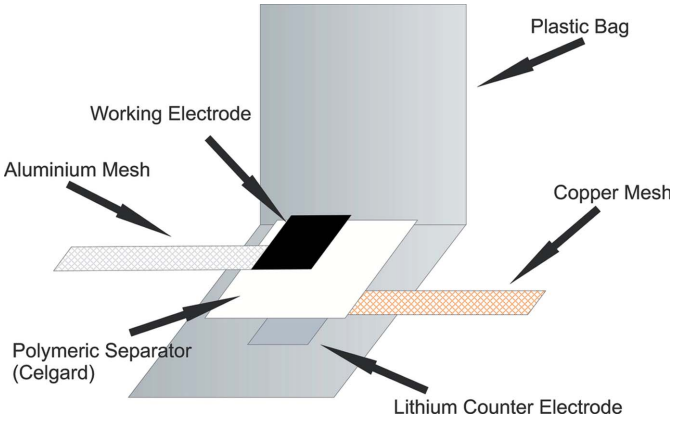

Figure 1
Schematic view of the 'coffee bag' type cell before sealing.

Figure 2
The two types of 'coffee bag' cells. On the left is the standard cell sealed in the machine; on the right the cell with a straw, sealed by hand.

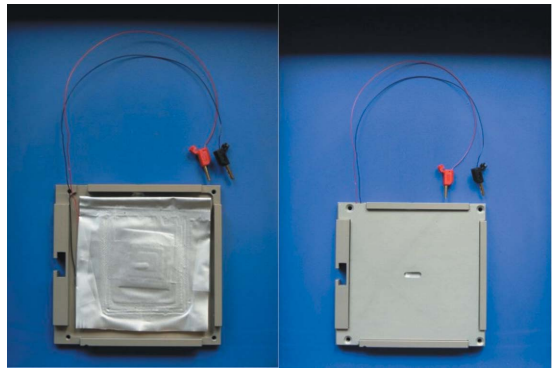

Figure 3
The 'coffee bag' cell enclosed in the holder (left without the cover). The X-rays pass through the small oval hole in the middle of the cell holder.

Table 1
Main characteristics of the MS beamline (Schmitt *et al.*, 2003).

Energy range	5–40 keV
Energy resolution	1.4×10^{-4} at 5 keV
Vertical divergence	0.2 mrad
Intensity	10^{13} photons s^{-1} on sample

allows for adjustable pressure on the cell elements as required. Wires are soldered to the current collectors and the contacts are protected with a plastic isolating foil to avoid short-circuiting.

2.2. Sample changer

The sample changer has been developed completely in house. It allows moving up to 32 cells into and out of the beam. It works using a 'slideshow motion'; the cells are placed on a sliding carriage that moves in discrete steps. When the cell that is to be measured is in the correct position, a compressed-air-operated slider pushes the cell holder into the beam. When the collection of the diffraction pattern is completed, the cell holder is retracted into the carriage and the procedure is repeated for the next cell. Apart from the standard 'coffee bag' cells, the sample changer can accommodate any other type of experimental cells; the only condition is the cell thickness. In Fig. 4 the sample changer mounted in the beamline hatch is shown with one of these special cells.

The sample changer is software-controlled from the beamline control hutch *via* a BASH shell script. The software is linked with both the software controlling the electrochemical measurements and the software controlling the X-ray data collection.

2.3. Beamline set-up

The measurements have been carried out at the MS beamline (X04SA) at the SLS in Villigen, Switzerland. The main beamline characteristics are summarized in Table 1.

At the beamline a powder diffractometer with two detector systems (a conventional analyzer set-up and the MYTHEN microstrip detector) is implemented as shown in Fig. 5. The advantage of the powder diffractometer of the SLS beamline over similar instruments at other synchrotron facilities is the MYTHEN microstrip detector. This detector with 15360 channels allows a fast readout time of 250 µs; this reduces the time needed for a pattern acquisition to seconds. The powder diffractometer also shows excellent resolution, as summarized in Table 2.

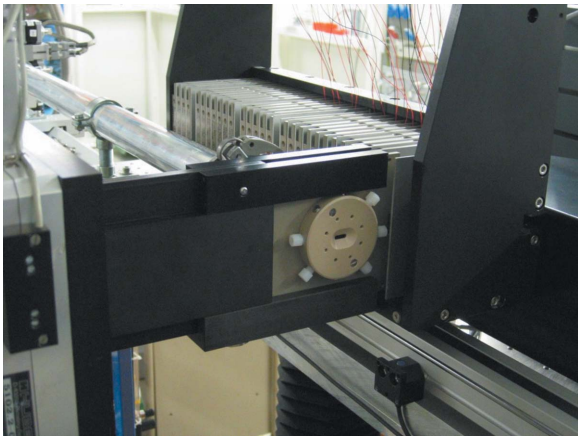

Figure 4
The sample changer at the MS beamline. The X-rays come from the tube at the back of the cell. A special experimental cell is shown in the beam position.

Table 2
Main characteristics of the MYTHEN detector system.

Angular convergence	60°
Intrinsic angular resolution	0.04°
Strip pitch	50 µm
Strip length	8 mm
Number of channels	15360
Readout time	250 µs

3. Examples of measurements

To demonstrate the possibilities of our system, two test cases were selected: (i) lithium de-intercalation during the first charge of a $LiCoO_2$ positive battery electrode, and (ii) the side reaction of co-intercalation of an ionic liquid into a SFG44 graphite negative electrode. All XRD measurements were performed using X-rays with an energy of 17.5 keV (λ = 0.7084 Å). This value has been chosen to minimize the effects of absorption by aluminium while preserving a high intensity of the beam.

3.1. $LiCoO_2$

$LiCoO_2$ is the standard material used in positive electrodes of lithium-ion batteries because of its high potential (∼4 V *versus* Li^+/Li), fairly high specific charge (∼160 mAh g^{-1}) and excellent cycling stability.

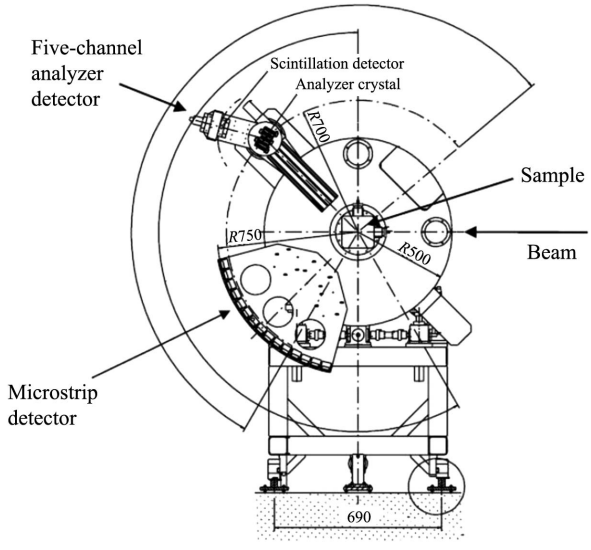

Figure 5
The powder diffractometer set-up at the MS beamline at the SLS. Image courtesy of the beamline team.

It has a layered rock salt structure and belongs to the $R\bar{3}m$ rhombohedral space group. Its crystalline structure is shown in Fig. 6. Upon charging, lithium ions are de-intercalated from the lithium-containing layers in $LiCoO_2$ (Mizushima *et al.*, 1980). On repeated cycling this material should normally not be de-intercalated further than *ca* $Li_{0.5}CoO_2$ in commercial batteries; a lesser lithium content causes the structure to be too unstable.

Previous experiments have shown (Ohzuku & Ueda, 1994) that upon delithiation the rhombohedral structure of $Li_{1-x}CoO_2$ evolves to a monoclinic lattice when $x \simeq 0.45$ is reached. In our experiment the delithiation of $LiCoO_2$ from the open circuit potential of *ca* 3 V to 4.8 V *versus* Li/Li^+ was followed. A total of 38 X-ray diffraction patterns were collected while the cell was charged with a constant current at the C-rate of C/10 (*i.e.* 10 h for a complete charge). The pattern evolution is visible from Fig. 7: the topmost pattern is from the oxide in the starting state, while the pattern at the bottom is from the oxide after charging the battery. It is possible to see the shift to lower angles of the (003) rhombohedral peak that indicates an enlargement of the *c*-axis of the unit cell of $LiCoO_2$, and, at around 4.4 V, the appearance of a new peak assigned to the (001) reflection of the new monoclinic phase. This peak stems from the (003) feature and splits completely from it.

A more striking feature is the change of the (002) reflection of carbon. (Carbon is present in the electrode as conductivity enhancer and is expected to be inactive.) It has been previously shown (Seel & Dahn, 2000) that at highly positive potentials the PF_6^- ions from the electrolyte solution can intercalate between the graphene sheets, thus enlarging the distance between the layers. When the potential becomes very positive the (002) peak of carbon loses intensity and then suddenly shifts to lower angles, indicating the intercalation of anions.

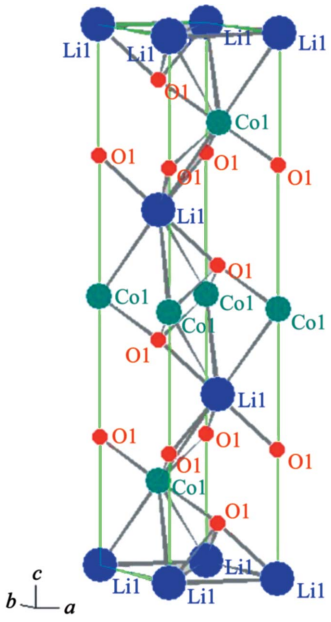

Figure 6
The $LiCoO_2$ structure.

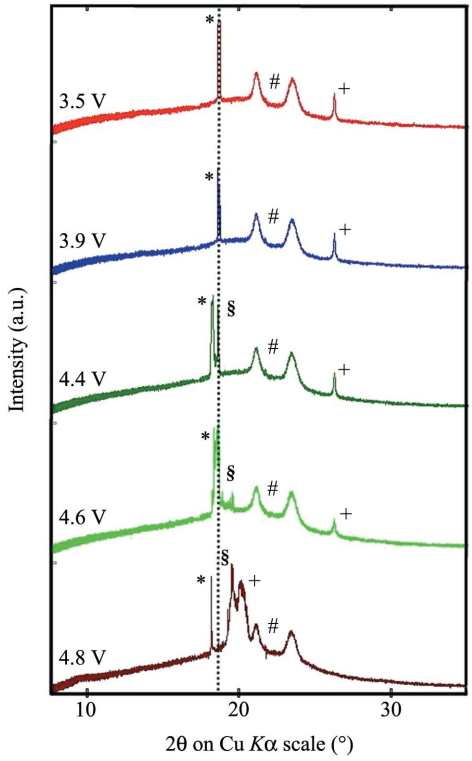

Figure 7
X-ray diffraction patterns evolution upon delithiation of $LiCoO_2$ in electrolyte ethylene carbonate : dimethyl carbonate (1 : 1) with 1 *M* $LiPF_6$. The indicated potential is *versus* Li/Li^+; the dotted line represents the position of the (003) rhombohedral peak. Peaks indicated are the (003) reflection of rhombohedral $Li_{1-x}CoO_2$ (*); the (002) reflection of carbon (+); the (001) reflection of monoclinic $Li_{1-x}CoO_2$ (§); and reflections from polyethylene and polypropylene from the cell case (#).

3.2. Ionic liquids

Ionic liquids are a new class of compounds that are investigated as a possible replacement for the standard non-aqueous electrolytes for lithium-ion batteries. Certain ionic liquids are stable up to potentials higher than 5 V *versus* Li^+/Li (Fernicola *et al.*, 2006). At negative potentials their use has been restricted up to now, as they are not thermodynamically stable at low potentials. But using pyrrolidinium-based ionic liquids (Howlett *et al.*, 2004) or film-forming additives (Zhang, 2006) may help to overcome these challenges and allows the reversible intercalation of lithium into, for example, graphite negative electrodes. However, a side reaction may occur which is the co-insertion into carbon of the cations from the ionic liquid itself at low potentials. The following experiment was designed to check for the possible intercalation behavior of the 1-ethyl-3-methylimidazolium cation (EMI^+) into graphite, using 1-ethyl-3-methylimidazolium tetrafluoroborate ($EMIBF_4$) as ionic liquid (McEwen *et al.*, 1999) electrolyte. The ion intercalation into graphite can be easily followed by studying the shift of the (002) peak. This reflection is related to the spacing between the graphene sheets, and a shift of the peak position to lower angles indicates an increase in the distance between the layers due to the ion and/or solvent (co-)intercalation. In Fig. 8 a series of 80 XRD measurements

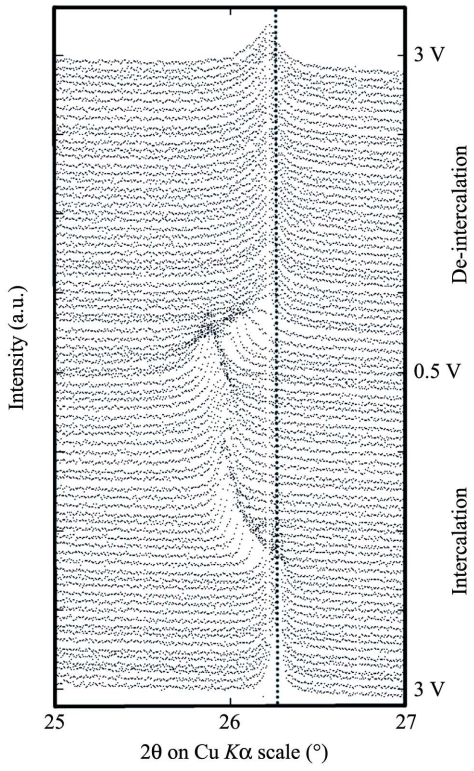

Figure 8
XRD patterns evolution following ethylmethylimidazolium intercalation and de-intercalation into/from graphite. All indicated potentials are *versus* Li/Li^+. The potential scan starts from 3 V for the bottom pattern, decreases to 0.5 V for the middle one, and goes back to 3 V for the top-most pattern. The counter electrode is activated carbon, the electrolyte is ethylene carbonate:dimethyl carbonate (1:1) with 1 *M* $LiPF_6$.

over 6 h is shown. Cyclic voltammetry was performed on the cell between the limits of 3 V and 0.5 V *versus* Li^+/Li, with no reference electrode, at a scan rate of 0.25 mV s^{-1} in ethylene carbonate:dimethylcarbonate (1:1) with 1 *M* $LiPF_6$ electrolyte.

The shift in the (002) peak position is clearly visible and quite reversible. Moreover, a certain peak broadening can be observed by comparing the first and the last pattern; this is probably due to irreversible structural disorder induced by the intercalation of large ions such as EMI^+.

4. Conclusion

A complete automatic system to perform multiple electrochemical *in situ* X-ray powder diffraction measurements at a synchrotron has been developed and successfully tested. The selected examples demonstrate how multiple patterns can be acquired repeatedly and how the collected data may be used for successive crystallographic and electrochemical evaluation: in the first example the appearance of the monoclinic phase after delithiation of rhombohedral $LiCoO_2$ and the intercalation effect of PF_6^- ions in graphite; in the second example the shift in the (002) graphite peak upon insertion of EMI^+ ions in the graphitic layered structure.

We are thankful to the MS beamline team at the SLS, namely Dr B. Schmitt and Dr D. Maden, for their help in setting up the system, and Gruber Folien GmbH for providing the layered foil.

References

Fernicola, A., Scrosati, B. & Ohno, H. (2006). *Ionics*, **12**, 95–102.
Gustafson, T., Thomas, J. O., Koksbang, R. & Farrington, G. C. (1992). *Electrochim. Acta*, **37**, 1639–1643.
Howlett, P. C., MacFarlane, D. R. & Hollenkamp, A. F. (2004). *Electrochem. Solid State Lett.* **7**, A97–A101.
McEwen, A. B., Ngo, H. L., LeCompte, K. & Goldman, J. L. (1999). *J. Electrochem. Soc.* **146**, 1687–1695.
Mizushima, K., Jones, P. C., Wiseman, P. J. & Goodenough, J. B. (1980). *Mater. Res. Bull.* **15**, 783–789.
Nishi, Y. (2001). *Chem. Rec.* **1**, 406–413.
Ohzuku, T. & Ueda, A. (1994). *J. Electrochem. Soc.* **141**, 2972–2977.
Schmitt, B., Brönnimann, C., Eikenberry, E. F., Gozzo, F., Hörmann, C., Horisberger, R. & Patterson, B. (2003). *Nucl. Instrum. Methods Phys. Res. A*, **501**, 267–272.
Seel, J. A. & Dahn, J. R. (2000). *J. Electrochem. Soc.* **147**, 892–898.
Tarascon, J. M. & Armand, M. (2001). *Nature (London)*, **141**, 359–367.
Tarascon, J. M., Godzd, A. S., Schmutz, C., Shokoohi, F. & Warren, P. C. (1996). *Solid State Ion.* **86–88**, 49–54.
Winter, M., Besenhard, J. O., Spahr, M. E. & Novák, P. (1998). *Adv. Mater.* **10**, 725–763.
Zhang, S. S. (2006). *J. Power Sources*, **162**, 1379–1394.